AIP | Conference Proceedings

Quasi-contiguous approximation for line-shape modeling in plasmas

E. Stambulchik and Y. Maron

Citation: AIP Conf. Proc. **1438**, 203 (2012); doi: 10.1063/1.4707878
View online: http://dx.doi.org/10.1063/1.4707878
View Table of Contents: http://proceedings.aip.org/dbt/dbt.jsp?KEY=APCPCS&Volume=1438&Issue=1
Published by the AIP Publishing LLC.

Quasi-Contiguous Approximation for Line-Shape Modeling in Plasmas

E. Stambulchik and Y. Maron

Faculty of Physics, Weizmann Institute of Science, Rehovot 76100, Israel

Abstract. We present an analytical method for the calculation of shapes of Stark-broadened spectral lines in plasmas, applicable to hydrogen and hydrogen-like transitions (including Rydberg ones). The method is based on the recently suggested quasi-contiguous approximation of the static Stark line shapes [E. Stambulchik, and Y. Maron, *J. Phys. B: At. Mol. Opt. Phys.* **41**, 095703 (2008)], while the dynamical effects are accounted for using the frequency-fluctuation-model approach. Comparisons with accurate computer simulations show excellent agreement.

Keywords: Stark broadening, line shapes, quasi-contiguous approximation, frequency fluctuation model, computer simulations.
PACS: 32.30.-r,32.60.+i

INTRODUCTION

Line shapes of hydrogen and hydrogen-like transitions (including Rydberg ones) are important for many topics of plasma physics and astrophysics. However, rigorous Stark broadening calculations of such lines are complex and time consuming. To overcome the difficulties, a simple analytical method for the calculation of line broadening was recently suggested [1], based on the quasi-contiguous (QC) approximation of the static Stark line shapes. With further accounting for the static and dynamic properties of the plasma micro-fields, a simple expression for the full width at half-maximum (FWHM) of the Stark line broadening in plasma was obtained. A very good accuracy was achieved over a range of transitions, species, and plasma parameters. Although the method is especially suitable for transitions with $\Delta n \gg 1$, it describes rather well even first members of the spectroscopic series with Δn as low as 2.

In this study, the QC method is extended to analytical calculations of line *shapes* (not mere line *widths*) in plasmas. To this end, we employ a recent formulation [2, 3] of the frequency fluctuation model (FFM).

METHOD

The detailed description of the QC approximation is given in Ref. [1]. For convenience, an abridged version is provided below. Furthermore, for the sake of simplicity, plasma is assumed ideal (no correlation effects), with all particles having equal temperature T.

Let us consider a dipole radiative transition between degenerate (hydrogen-like or Rydberg) levels with the principal quantum numbers n and n'. The line shape of the

The 17th International Conference on Atomic Processes in Plasmas (ICAPiP)
AIP Conf. Proc. 1438, 203-209 (2012); doi: 10.1063/1.4707878

transition can be factorized as

$$I_{\rm qs}(\omega) = I^{(0)}_{nn'} L_{\rm qs}(\omega), \tag{1}$$

where $I^{(0)}_{nn'}$ is the total line intensity and ω is assumed relative to the zero-field line position ω_0. It is convenient to re-write the area-normalized line-shape $L_{\rm qs}(\omega)$ using the reduced detuning $\bar{\omega} = \omega/\Delta_0$, where

$$\Delta_0 = \alpha_{nn'} F_0/\hbar\ . \tag{2}$$

Here, F_0 is the Holtsmark normal field strength [4]

$$F_0 = 2\pi\,(4/15)^{2/3}\,Z_{\rm p} e N_{\rm p}^{2/3} \tag{3}$$

and $\alpha_{nn'}$ is the linear-Stark-effect coefficient:

$$\alpha_{nn'} = \frac{3}{2}(n^2 - n'^2)\frac{e a_0}{Z}\ . \tag{4}$$

In the expressions above, $\hbar$ is the reduced Plank constant, e is the elementary charge, a_0 is the Bohr radius, Z is the core charge of the radiator (in units of e), and $Z_{\rm p}$ and $N_{\rm p}$ are, respectively, the charge and the density of the perturber particles.

As shown in [1], for $n - n' \gg 1$ the quasistatic line shape can be accurately approximated by

$$L_{\rm qs}(\bar{\omega}) = S(\bar{\omega}), \tag{5}$$

where the S function is analytically defined as

$$S(\bar{\omega}) = \frac{1}{\pi}\int_0^\infty \cos(\bar{\omega}x)\exp(-x^{3/2})\mathrm{d}x\ . \tag{6}$$

Defining its half width at half maximum (HWHM) as $\bar{\omega}^0_{1/2} \approx 1.44$, one can write the quasistatic FWHM as

$$w_{\rm qs} = 2\bar{\omega}^0_{1/2}\Delta_0\ . \tag{7}$$

Accounting for the influence of the micro-field dynamics on the line width is done by introducing a "quasistaticity" factor f, defined as

$$f = \frac{R}{R + R_0}, \tag{8}$$

where

$$R = \frac{w_{\rm qs}}{w_{\rm dyn}} \tag{9}$$

is the ratio of the quasistatic width to the typical frequency of the micro-field fluctuations $w_{\rm dyn}$,

$$w_{\rm dyn} = \frac{\langle v\rangle}{\langle r\rangle} = \sqrt{\frac{kT}{m_{\rm p}^*}}\left(\frac{4\pi N_{\rm p}}{3}\right)^{1/3}\ . \tag{10}$$

Here, m_p^* is the reduced mass of the perturbers. The dimensionless constant R_0, determining transition from the quasistatic to dynamic regime, was inferred by comparisons with computer simulation results and found to be 0.5.

The full dynamic Stark width is then

$$w = f w_{qs}. \tag{11}$$

We note that the semi-empiric treatment of dynamic effects by Eqs. (8–11) has two important properties: (i) it gives the correct quasistatic width in the high-density/low-temperature limit and (ii) reproduces the expected T- and N_p-dependences in the low-density/high-temperature impact limit [5],

$$w \propto N_p/\sqrt{T}. \tag{12}$$

A recent formulation [2, 3] of the original FFM approximation [6] is an attractive approach for very fast line-shape calculations. The dynamic line-shape is a functional of the quasistatic profile $L_{qs}(\omega)$:

$$L(\nu;\omega) = \frac{1}{\pi}\mathrm{Re}\,\frac{\int \frac{L_{qs}(\omega')\mathrm{d}\omega'}{\nu+i(\omega-\omega')}}{1-\nu\int \frac{L_{qs}(\omega')\mathrm{d}\omega'}{\nu+i(\omega-\omega')}}, \tag{13}$$

where

$$\nu = C_0\, w_{dyn} \tag{14}$$

and C_0, similarly to R_0 in Eq.(8), is to be determined empirically by comparisons with computer simulation results [7].

The important features of Eq. (13) are: (i) it preserves normalization, $\int L(\omega)\mathrm{d}\omega = 1$; (ii) it recovers the quasistatic limit, i.e., at $\nu \to 0, L(\omega) \to L_{qs}(\omega)$; and (iii) far wings of the line-shape remain quasistatic: $L(\omega) \to L_{qs}(\omega)$ for $|\omega| \gg \nu$.

Equation (13) can be re-written as a function of the reduced detuning $\bar{\omega}$:

$$L(\bar{\nu};\bar{\omega}) = \frac{1}{\pi}\mathrm{Re}\,\frac{J(\bar{\nu};\bar{\omega})}{1-\bar{\nu}J(\bar{\nu};\bar{\omega})}, \tag{15}$$

where $\bar{\nu} = \nu/\Delta_0$ and

$$J(\bar{\nu};\bar{\omega}) \equiv \int \frac{L_{qs}(\bar{\omega'})\mathrm{d}\bar{\omega'}}{\bar{\nu}+i(\bar{\omega}-\bar{\omega'})}. \tag{16}$$

The integral in Eq. (16) is a convolution of two functions, $L_{qs}(\bar{\omega})$ and $(\bar{\nu}+i\bar{\omega})^{-1}$, therefore, it can be represented as

$$J(\bar{\nu};\bar{\omega}) = \mathscr{F}\left\{\mathscr{F}^{-1}\{L_{qs}(\bar{\omega})\}\mathscr{F}^{-1}\left\{(\bar{\nu}+i\bar{\omega})^{-1}\right\}\right\}, \tag{17}$$

where $\mathscr{F}$ and $\mathscr{F}^{-1}$ designate the direct and inverse Fourier transforms, respectively. Noticing that for $\bar{\nu} > 0$

$$\mathscr{F}^{-1}\left\{(\bar{\nu}+i\bar{\omega})^{-1}\right\}(\tau) = e^{-\bar{\nu}\tau}\theta(\tau), \tag{18}$$

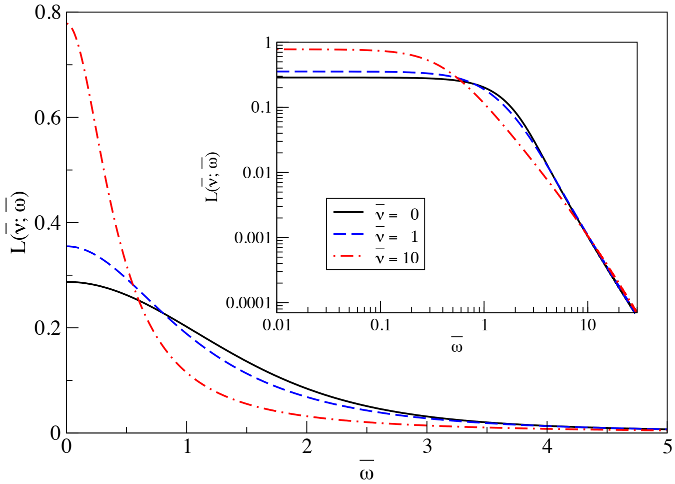

FIGURE 1. Line-shapes as given by Eq. (22) for different values of $\bar{\nu}$.

where $\theta(\tau)$ is the Heaviside step function ($\theta(\tau)$ is zero for negative τ and unity for positive τ), we obtain an alternative expression for $J(\bar{\nu};\bar{\omega})$ which will be more convenient for our purposes:

$$J(\bar{\nu};\bar{\omega}) = \int_0^\infty d\tau\, e^{-i(\bar{\omega}-i\bar{\nu})\tau} \mathscr{F}^{-1}\{L_{qs}\}(\tau)\ . \tag{19}$$

We now substitute the general quasistatic line-shape L_{qs} in Eq. (19) with the QC one (5). $S(\bar{\omega})$ is an even function, hence, its direct and inverse Fourier transforms are the same. Therefore, using Eq. (A.6) from [1],

$$J(\bar{\nu};\bar{\omega}) = \int_0^\infty d\tau \exp\left(-\tau^{3/2} - i(\bar{\omega}-i\bar{\nu})\tau\right) = T_{3/2}(\bar{\omega}-i\bar{\nu}), \tag{20}$$

where

$$T_\mu(z) \equiv \int_0^\infty d\xi \exp\left(-\xi^\mu - iz\xi\right)\ . \tag{21}$$

Therefore,

$$L(\bar{\nu};\bar{\omega}) = \frac{1}{\pi} \mathrm{Re}\, \frac{T_{3/2}(\bar{\omega}-i\bar{\nu})}{1-\bar{\nu}\, T_{3/2}(\bar{\omega}-i\bar{\nu})}\ . \tag{22}$$

Plots of $L(\bar{\nu};\bar{\omega})$ for $\bar{\nu} = 0, 1$, and 10 are given in Fig. 1. Evidently, $L(0;\bar{\omega})$ is exactly the quasistatic $S(\bar{\omega})$. For $\bar{\nu} = 1$, a deviation from the quasistatic profile is noticeable, and at $\bar{\nu} = 10$, the line becomes significantly narrower. Nevertheless, sufficiently far wings ($|\bar{\omega}| \gg \bar{\nu}$) remain quasistatic, clearly seen in the log-log scale shown in the inset of the figure.

Let us consider the line-shape in the collision-dominated limit, i.e., for $\bar{\nu} \gg 1$. The central part of the profile ($|\bar{\omega}|/\bar{\nu} \ll 1$) can be obtained by substituting in Eq. (22) $T_{3/2}(\bar{\omega}-i\bar{\nu})$ with first two terms of its Taylor series expansion, resulting in

$$L(\bar{\nu};\bar{\omega}) \simeq \frac{1}{\pi} \frac{\frac{\Gamma(5/2)}{\bar{\nu}^{1/2}}}{\left[\frac{\Gamma(5/2)}{\bar{\nu}^{1/2}}\right]^2 + \bar{\omega}^2}\ , \tag{23}$$

i.e., a Lorentzian with HWHM $\bar{\gamma} = \frac{\Gamma(5/2)}{\bar{\nu}^{1/2}}$, or, in the usual units,

$$\gamma = \Gamma(5/2)\Delta_0 \left(\frac{\Delta_0}{\nu}\right)^{1/2} . \tag{24}$$

Therefore,

$$\gamma \propto \frac{N_\mathrm{p}^{5/6}}{T^{1/4}} . \tag{25}$$

This result is in evident contradiction to the expected N_p- and T-dependence of the impact limit of the Stark broadening (12). Thus, the FFM dynamic correction, while providing an excellent route to fast and accurate line-shape calculations up to moderate values of $\bar{w}_\mathrm{dyn}$, fails in the $\bar{w}_\mathrm{dyn} \gg 1$ region.[1] It should be mentioned that for practical purposes, the region of applicability is, as a rule, absolutely adequate for ion perturbers, however, for electrons it is not necessarily so. While it is possible (and, indeed, often done this way) to include the electron broadening via a convolution with a Lorentzian of an appropriate width (calculated in the impact approximation), a universal analytical approach is evidently desired.

Here, we suggest to introduce an effective $\tilde{\nu}$, to be used in place of $\bar{\nu}$, satisfying the following requirements:

$$\tilde{\nu} \to \begin{cases} \bar{\nu} & , \ \bar{\nu} \ll 1 \\ \propto \bar{\nu}^2 & , \ \bar{\nu} \gg 1 \end{cases} , \tag{26}$$

with the line-shape given by

$$L(\bar{\nu};\bar{\omega}) = \frac{1}{\pi} \mathrm{Re} \frac{T_{3/2}(\bar{\omega} - i\tilde{\nu})}{1 - \tilde{\nu}\, T_{3/2}(\bar{\omega} - i\tilde{\nu})} . \tag{27}$$

Evidently, Eqs. (26) and (27) for $\bar{\nu} \gg 1$ give the correct impact-limit dependences:

$$\gamma \propto \Delta_0 \left(\frac{\Delta_0}{\nu}\right) \propto N_\mathrm{p}/\sqrt{T} . \tag{28}$$

An obvious choice for $\tilde{\nu}$ is

$$\tilde{\nu} = \bar{\nu} + \frac{\bar{\nu}^2}{\bar{\nu}_0} . \tag{29}$$

By comparison with the computer simulation [8] results, it was determined that $\bar{\nu}_0 \approx 5$ gives the best overall fit. However, varying the parameter twofold in each direction shows a rather minor sensitivity to specific value. The results of the comparison are given in Fig. 2, where a very good agreement is seen over the whole range of temperatures considered. The significant improvement vs. the non-corrected calculations is evident.

---

[1] The failure to approach the impact limit was already noted in the first FFM paper [6].

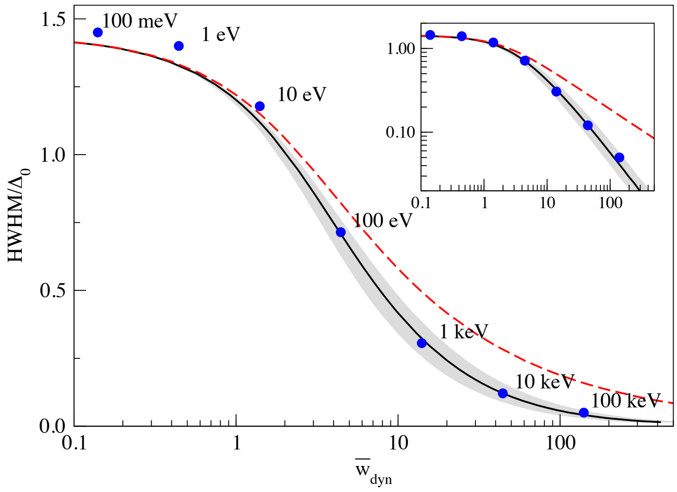

FIGURE 2. HWHM of the Stark broadening of H Lyδ due to proton perturbers with $N_p = 10^{14}\,\text{cm}^{-3}$. Debye screening is neglected. – – calculations according to Eq. (22); — calculations according to Eqs. (27) and (29) with $\bar{v}_0 = 5$, with the hashed area indicating results obtained by varying $\bar{v}_0$ between 2.5 and 10; • computer simulation results, annotated with the plasma temperature assumed.

EXAMPLES AND APPLICATIONS

As an example, given in Fig. 3a are calculation results for the shape of Lyman δ of H-like neon in a deuterium plasma with $N_e = 10^{21}$ cm^{-3} and $kT = 1000$ eV (such a plasma may exist in mega-ampere deuterium-puff z-pinches, with neon used as a dopant). The line shapes due to ions and electrons separately are shown by the dashed and dot-dashed curves, respectively, while the total line shape (solid line) is obtained by convolving these two shapes. For comparison, the line shape was also calculated using a computer simulation method [8][2] assuming the same plasma conditions[3], shown by the circle symbols. An excellent agreement over the entire line shape is evident, including the very far wings, where the line intensity falls by a few orders of magnitude relatively to its peak value; this is clearly seen in the log-log scale given in the inset of the figure. We also note that the asymptotic behavior of the far wings due to electrons is the same as that due to (singly charged) ions, as expected.

Another example is given in Fig. 3b, where results of calculations for the deuterium $n = 9$ Balmer line for $N_e = 5 \times 10^{14}\,\text{cm}^{-3}$ and $kT = 4\,\text{eV}$ (conditions typical for magnetic fusion experiments) are presented. Here again, a very good ($< 10\%$) agreement with the computer-simulation results is demonstrated over the entire line shape.

These examples demonstrate the applicability of the new method to a broad range of scientifically sound cases. The calculations are very fast, therefore, it becomes practical to incorporate them, into non-LTE plasma kinetics codes (e.g., [10, 11]), compromising

[2] The agreement with other calculations and, where available, with experimental data was shown to be very good, see, e.g., [9].

[3] In the derivation, we assumed an ideal plasma, therefore, in order to make the comparison justified, straight-line trajectories of unshielded (Coulomb) particles were used in the simulations in this study.

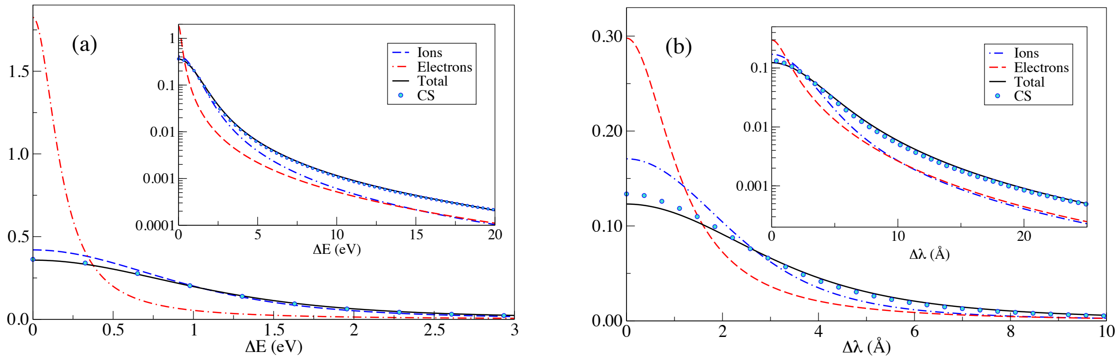

FIGURE 3. Comparison between analytical and computer simulation (CS) results of Stark broadening of a) Ne X Lyδ in deuterium plasma with $N_e = 10^{21}\,\text{cm}^{-3}$ and $kT = 1\,\text{keV}$; b) D Balmer $n = 9$ line in deuterium plasma with $N_e = 5\times10^{14}\,\text{cm}^{-3}$ and $kT = 4\,\text{eV}$.

neither accuracy nor computational resources required. Furthermore, the computational time is independent of the principal quantum numbers of the transitions involved, therefore, the method can be easily applied to such complex phenomena as merging of the discrete and continuum spectra and ionization potential lowering due to plasma effects. Such calculations are indeed planned to be used for the understanding of controlled measurements of line shape and continuum spectra of photoionized plasmas performed at Sandia National Laboratories (USA) [12].

ACKNOWLEDGMENTS

We gratefully acknowledge fruitful discussions with A. Calisti, H.R. Griem, J.D. Hey, and G.A. Rochau. This work was supported in part by the Israel Science Foundation, the Minerva Foundation (Germany), and Sandia National Laboratories (USA).

REFERENCES

1. E. Stambulchik, and Y. Maron, *J. Phys. B: At. Mol. Opt. Phys.* **41**, 095703 (2008).
2. A. Calisti, C. Mossé, S. Ferri, B. Talin, F. Rosmej, L. A. Bureyeva, and V. S. Lisitsa, *Phys. Rev. E* **81**, 016406 (2010).
3. L. A. Bureeva, M. B. Kadomtsev, M. G. Levashova, V. S. Lisitsa, A. Calisti, B. Talin, and F. Rosmej, *JETP Letters* **90**, 647–650 (2010).
4. J. Holtsmark, *Ann. Phys. (Leipzig)* **58**, 577–630 (1919).
5. H. R. Griem, *Spectral line broadening by plasmas*, Academic Press, New York, 1974, ISBN 0-12-302850-7.
6. B. Talin, A. Calisti, L. Godbert, R. Stamm, R. W. Lee, and L. Klein, *Phys. Rev. A* **51**, 1918–1928 (1995).
7. A. Calisti, private communication (2011).
8. E. Stambulchik, and Y. Maron, *J. Quant. Spectr. Rad. Transfer* **99**, 730–749 (2006).
9. E. Stambulchik, S. Alexiou, H. R. Griem, and P. C. Kepple, *Phys. Rev. E* **75**, 016401 (2007).
10. Y. V. Ralchenko, and Y. Maron, *J. Quant. Spectr. Rad. Transfer* **71**, 609 (2001).
11. V. Fisher, D. Fisher, and Y. Maron, *High Energy Density Phys.* **3**, 283 (2007).
12. G. A. Rochau, private communication (2011).